

Biochemical Characterization of the Two-Component Flavin-Dependent Monooxygenase Involved in Valanimycin Biosynthesis

Hao Li, Benedicta Forson, Meital Eckshtain-Levi, Hannah Valentino, Julia S. Martín del Campo, John J. Tanner, and Pablo Sobrado*



Cite This: *Biochemistry* 2021, 60, 31–40



Read Online

ACCESS |



Metrics & More

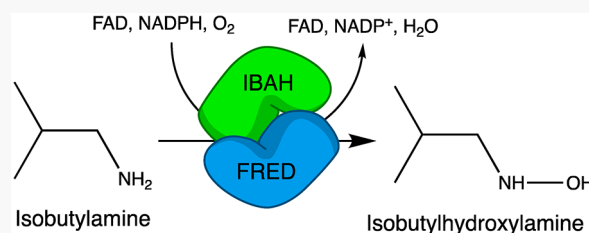


Article Recommendations



Supporting Information

ABSTRACT: The flavin reductase (FRED) and isobutylamine *N*-hydroxylase (IBAH) from *Streptomyces viridifaciens* constitute a two-component, flavin-dependent monooxygenase system that catalyzes the first step in valanimycin biosynthesis. FRED is an oxidoreductase that provides the reduced flavin to IBAH, which then catalyzes the hydroxylation of isobutylamine (IBA) to isobutylhydroxylamine (IBHA). In this work, we used several complementary methods to investigate FAD binding, steady-state and rapid reaction kinetics, and enzyme–enzyme interactions in the FRED:IBAH system. The affinity of FRED for FAD_{ox} is higher than its affinity for FAD_{red}, consistent with its function as a flavin reductase. Conversely, IBAH binds FAD_{red} more tightly than FAD_{ox}, consistent with its role as a monooxygenase. FRED exhibits a strong preference (28-fold) for NADPH over NADH as the electron source for FAD reduction. Isothermal titration calorimetry was used to study the association of FRED and IBAH. In the presence of FAD, either oxidized or reduced, FRED and IBAH associate with a dissociation constant of 7–8 μM. No interaction was observed in the absence of FAD. These results are consistent with the formation of a protein–protein complex for direct transfer of reduced flavin from the reductase to the monooxygenase in this two-component system.



Flavin-dependent monooxygenases (FMOs) are involved in many important metabolic processes. This family of enzymes catalyzes the insertion of a single atom of oxygen into diverse substrates, many of which are precursors to molecules that have antibacterial or anticancer properties.¹ For monooxygenation, the key step is the activation of oxygen by the reduced flavin. This is accomplished by a single electron transfer step that leads to the formation of superoxide and a flavin semiquinone radical pair that collapses and generates a flavin-hydroperoxide intermediate (FAD_{OOH}).^{2,3}

The flavin-dependent monooxygenase family has been divided into eight classes based on activity and structural fold. Classes A, B, G, and H, which have been well-studied, are single-component flavoprotein monooxygenases. Groups A and B contain both an NADPH and flavin-binding domains, allowing flavin reduction and substrate oxidation to occur in a single protein. Groups G and H contain a flavin-binding domain and obtain reducing equivalents from the substrate that is oxidized. Classes C–F are the two-component flavin-dependent monooxygenase systems. These consist of two enzymes: a reductase, which reduces the flavin, and a monooxygenase that utilizes the reduced flavin as a substrate for monooxygenation reactions.^{4,5} Examples of two-component monooxygenases that utilize FMN or FAD as cofactors are *p*-hydroxyphenylacetate hydroxylase (HPAH) from *Acinetobacter baumannii*,⁶ phenol hydroxylase from *Bacillus thermoglucosidarius*,⁷ and styrene monooxygenase from *Pseudomonas fluorescens*.⁸

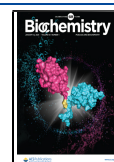
An interesting aspect of the mechanism of two-component monooxygenases is how the reduced flavin is transferred from the reductase to the monooxygenase. One proposed mechanism is the direct transfer of the reduced flavin via the formation of a protein–protein complex. This idea is supported by biochemical data and docking studies based on X-ray structures of reductases and monooxygenases.^{9–15} Alternatively, it has been suggested that flavin transfer occurs via free diffusion from the reductase to the monooxygenase, without the necessity for protein–protein interaction.^{16–18}

In this study, we focused on the biochemical characterization of the two-component monooxygenase system involved in the biosynthesis of the antibiotic valanimycin, a naturally occurring azoxy compound isolated from *Streptomyces viridifaciens* MG456-hF10.¹⁹ Valanimycin biosynthesis includes decarboxylation of *L*-valine, forming isobutylamine (IBA), which is hydroxylated and then reacted with *L*-serine. It has been shown that a key step in valanimycin biosynthesis is the conversion of isobutylamine to isobutylhydroxylamine (IBHA), which is catalyzed by a two-component flavin-dependent monooxyge-

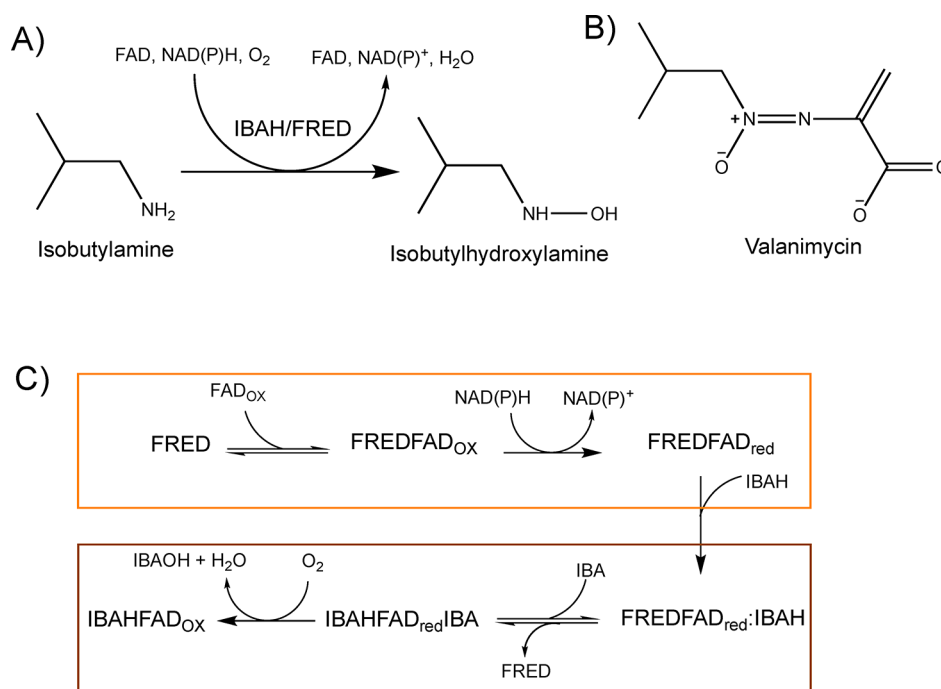
Received: August 13, 2020

Revised: December 14, 2020

Published: December 22, 2020



Scheme 1. (A) Reaction Catalyzed by the FRED:IBAH System, (B) Structure of Valanimycin, and (C) Catalytic Cycle of the FRED:IBAH System^a



^aReduction of the flavin by FRED occurs in the reductive-half reaction (orange). After transfer of the reduced flavin to IBAH, oxygen activation, and IBA binding, the hydroxylation occurs in the oxidative half-reaction (brown). Our data suggest that upon binding FAD, FRED transfers the reduced FAD upon forming a complex with IBAH.

nase (Scheme 1).^{20,21} Similar to other two-component systems, the monooxygenase in valanimycin biosynthesis cooperates with a flavin reductase (FRED), which provides reduced flavin for isobutylamine *N*-hydroxylase (IBAH) (Scheme 1). Crystal structures of IBAH and FRED are currently not available. IBAH is predicted to have the acyl-CoA dehydrogenase fold. The closest homologue of IBAH in the Protein Data Bank (PDB) is dibenzothiophene monooxygenase (PDB entry 3X0Y, 26% identical).²² FRED has only one detectable relative in the PDB, PheA2 (PDB entry 1RZ1, 30% identical), which is the flavin reductase component of a two-component monooxygenase system involved in the conversion of phenol to catechol.²³ Herein, we report a detailed study of the ligand binding and kinetics of the FRED:IBAH system, which reveals insight into the catalytic mechanism. Our data are consistent with direct transfer of reduced FAD from FRED to IBAH.

EXPERIMENTAL PROCEDURES

Materials. Synthetic genes encoding isobutylamine *N*-hydroxylase (IBAH) and flavin reductase (FRED) from *S. viridifaciens* were obtained from Genscript (Piscataway, NJ), and *Escherichia coli* Turbo BL-21(DE3) chemically competent cells from Invitrogen (Waltham, MA). Protein purification was carried out on an AKTA Prime Plus Fast Protein Liquid Chromatography (FPLC) instrument from GE Healthcare (Chicago, IL). IBA was obtained from Sigma-Aldrich (St. Louis, MO), and NADPH, NADH, NADP⁺, NAD⁺, buffers, and salts were from Fisher Scientific (Pittsburgh, PA).

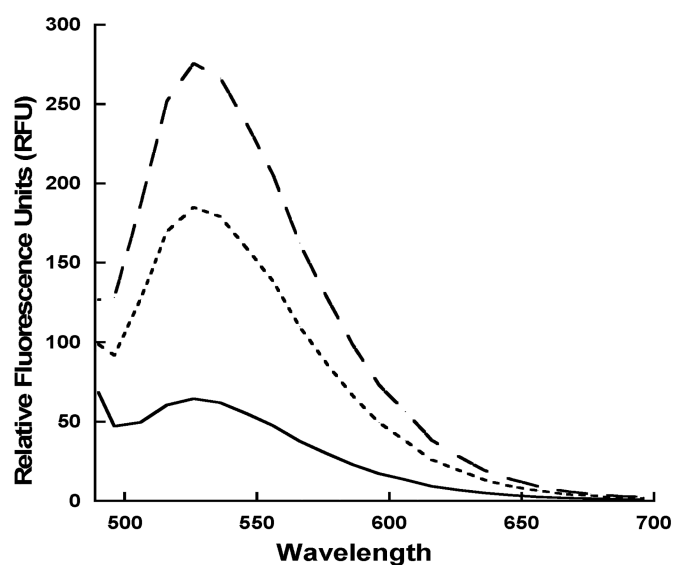
Protein Expression and Purification. The genes for both IBAH and FRED were subcloned into the pET15b plasmid for expression as N-terminal six-His fusion proteins. Chemically

competent *E. coli* Turbo BL-21(DE3) cells were transformed with pET15b_IBAH or pET15b_FRED, plated on an ampicillin (100 mg/mL)-containing agar plate, and incubated for 12 h at 37 °C. A single colony was used to inoculate 60 mL of lysogenic broth (LB) supplemented with ampicillin (100 mg/mL). This culture was incubated for ~12 h at 37 °C, and 6-fernbach flasks containing 1 L of autoinduction medium²⁴ were each inoculated with 10 mL of the cell culture. The 1 L cultures were incubated at 37 °C until the optical density at 600 nm reached a value of ~3, at which point the temperature was decreased to 20 °C and incubation extended for an additional 12 h. Cells were harvested by centrifugation at 4000g for 20 min, and the pellet was stored at -80 °C. This procedure yielded ~15 g of cells per liter of medium. For protein purification, we followed procedures established in our laboratory and previously published.^{25–27} The final protein yield was ~3 mg of purified protein per gram of cells. The protein samples were >95% pure, as evaluated by sodium dodecyl sulfate–polyacrylamide gel electrophoresis (SDS–PAGE) (Figure S1). The proteins were stored in 100 mM sodium phosphate buffer (pH 7.5) at -80 °C.

Oxygen Consumption Assays. The oxygen consumption activity was monitored using a Hansatech (Norfolk, England) oxygen monitoring system. The reaction with 10 μM FAD, 2 μM IBAH, and 50 nM FRED was initiated after addition of NADPH to the final volume of 1 mL of 100 mM sodium phosphate buffer (pH 7.5). In assays in which IBA concentrations were varied, 1 mM NADPH was used, and 5 mM IBA was used when NADPH concentrations were varied.

Isobutylamine Hydroxylation Assay. The amount of hydroxylated product formed by the FRED:IBAH system was determined with a variation of the Csaky iodine oxidation reaction.^{25,26,28,29} In this assay, hydroxylamines are oxidized to

(A)



(B)

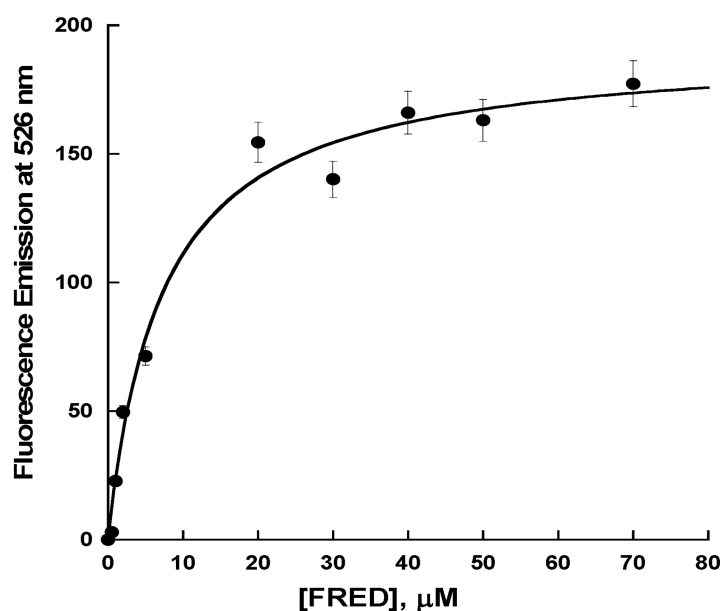


Figure 1. FAD binding to FRED. (A) Effect of FAD fluorescence upon addition of FRED [0 μM (solid line), 10 μM (short dashes), and 20 μM (long dashes)]. (B) Fluorescence intensity at 526 nm plotted as a function of FRED concentration (0.2–70 μM). The reaction was performed in 50 mM Tris-HCl buffer (pH 8.0) at 25 $^{\circ}\text{C}$, with a cutoff of 455 nm.

nitrite. Nitrite is detected by reaction with sulfanilic acid to form a diazonium salt. Addition of α -naphthylamine generates a strongly absorbing azo dye, which is detected spectrophotometrically at 562 nm. The solutions consisted of 107 μL of 100 mM sodium phosphate (pH 7.5) and concentrations of IBA or NADPH ranging from 0 to 20 mM and from 0 to 1 mM, respectively. In assays that were performed with varying amounts of IBA, NADPH was present at a concentration of 0.8 mM and FAD at a concentration of 10 μM . In assays that were performed with varying amounts of NADPH, IBA concentrations were kept constant at 3 mM and FAD concentrations at 10 μM . The reaction mixtures contained 50 nM FRED, and the reactions were initiated by addition of IBAH (2 μM) and

allowed to proceed for 5 min at 30 $^{\circ}\text{C}$. The reaction was quenched with the addition of 52.5 μL of 2 N perchloric acid. Aliquots (47.5 μL each) of the terminated reaction mixture were transferred into a 96-well plate for color development. The pH values of the reaction mixtures were neutralized by the addition of 47.5 μL of a 10% (w/v) sodium acetate solution, followed by the addition of 47.5 μL of 1% (w/v) sulfanilic acid in 25% (v/v) acetic acid. Then, 19 μL of 0.5% (w/v) iodine in glacial acetic acid was added, and the reaction mixture was incubated at 25 $^{\circ}\text{C}$ for 15 min. Excess iodine was removed by the addition of 19 μL of 0.1 N sodium thiosulfate, and the color was developed via addition of 19 μL of 0.6% (w/v) α -naphthylamine in 30% (v/v) acetic acid. After incubation for 5

min, the absorbance at 562 nm was recorded on a SpectraMax M5 plate reader (Molecular Devices). A standard curve of hydroxylamine hydrochloride was used to calculate the amount of hydroxylated product.

Flavin Binding Measured by Fluorescence. The binding of FAD to flavin reductase was assessed by monitoring the changes in flavin fluorescence at 526 nm (excitation at 450 nm) on a SpectraMax M5e plate reader (Molecular Devices, Sunnyvale, CA). The reaction was carried out in 25 μ L of 50 mM Tris-HCl buffer (pH 7.0). The reaction mix consisted of 10 μ M FAD and varying concentrations of FRED (0.2–70 μ M). The affinity of FAD for FRED was determined by measuring the change in fluorescence and fitting the data to eq 1.

$$\text{fluorescence} = \frac{[E]_T + [FAD]_T + K_D - \sqrt{([E]_T + [FAD]_T + K_D)^2 - 4[E]_T[FAD]_T}}{2} \quad (1)$$

Identification of Hydroxybutylamine. To analyze the incorporation of oxygen into IBA, reaction mixtures were derivatized with fluorenylmethyloxycarbonyl chloride (FMOC-Cl) to facilitate separation and detection using HPLC. Mass spectrometry was used to confirm the identity of the product. FMOC-Cl, which reacts with primary amines, was used to generate derivatives of IBA and IBHA to allow monitoring at 263 nm. The reaction mixture consisted of 100 μ L of 50 mM Tris-HCl buffer (pH 8.0) containing 20 μ M IBAH, 0.5 μ M FRED, 2 mM NADPH, 10 μ M FAD, and 1 mM IBA, and the reaction was stopped with 30% acetonitrile after incubation for 5 min. FMOC-Cl (5 mM) was then added, and the reaction mixture was incubated for 5 min. Excess FMOC-Cl was removed by addition of 1-aminoadamantane (50 mM) and incubated for an additional 15 min. An HPLC C18 column (250 mm \times 4.6 mm, 5 μ m) was utilized for the separation before ESI-MS analysis. The column was equilibrated in water and 0.1% formic acid. Reactions were analyzed using a flow rate of 1 mL/min. The samples were eluted with a linear gradient from 0% to 100% eluent B (acetonitrile and 0.15% formic acid). Column effluent was monitored using a diode array detector. Fractions were analyzed on an AB Sciex 3200 Qtrap mass spectrometer. Positive ions were detected over a mass range of 50–600 Da (at a rate of 1000 Da/s).

Flavin Reduction. The reduction of FAD bound to FRED was monitored using the single mixing mode in the stopped-flow spectrophotometer, with NADPH and NADH as reductants in the presence and absence of IBA. A FRED/FAD_{ox} solution (10 μ M each after mixing) was mixed with saturating concentrations of NAD(P)H (4 mM, final concentrations after mixing) in the presence or absence of 3 mM IBA. FAD reduction was recorded by following the decrease in absorbance at 450 nm. Measurements were recorded on a logarithmic scale, in triplicate. The observed rate constants were determined using KaleidaGraph (Synergy Software, Reading, PA) by fitting the data to a single-exponential decay equation.

Flavin Reoxidation in the Absence of a Substrate. Flavin reoxidation was monitored in the absence of IBA. The reoxidation was carried out in a single-mixing mode on the stopped-flow instrument. In one syringe, FAD (20 μ M after mixing) was mixed with IBAH (3 equiv), FRED (0.1 equiv), and NADPH (1.1 equiv). The mixture was incubated for 10 min to ensure complete reduction of the FAD, which was

confirmed by the stopped-flow spectrum. The completely reduced FAD was reacted with molecular oxygen (\sim 625 μ M after mixing). The reoxidation of FAD was monitored by observing the increase in absorbance at 450 nm. Stock aerobic buffer was prepared by bubbling 100% oxygen into 100 mM sodium phosphate buffer for 30 min at 4 $^{\circ}$ C (\sim 1.25 mM).

Isothermal Titration Calorimetry. The association of FAD_{ox/red} with IBAH or FRED, NAD(P)⁺ with FRED, and IBAH:FAD_{red} with FRED:FAD_{ox} were studied by isothermal titration calorimetry (ITC) measurements using an Auto-iTC 200 isothermal titration calorimeter (Malvern). Experiments were carried out in 50 mM sodium phosphate (pH 7.5). For experiments involving reduced FAD, the solution was prepared under anaerobic conditions, and 1–2 mM sodium dithionite (Na₂S₂O₄) was added to both the cell and the syringe solution to eliminate any trace of O₂. During titration, the reaction mixture was continuously stirred at 750 rpm and 25 $^{\circ}$ C. The thermodynamic parameters for the binding were determined from ITC results using Microcal Origin version 7.0 (Origin-Lab). FAD was present in both chambers at a concentration of 0.23 mM; the IBAH concentration was 0.23 mM, and the FRED concentration was 0.023 mM. Injection of a buffer containing only 0.023 mM FAD into IBAH (0.23 mM) was used as the blank.

RESULTS

Purification of IBAH and FRED. The purification of IBAH yielded 62.5 mg/L of a soluble and stable protein. The

Table 1. Kinetic Parameters for the NADPH Oxidase Activity of FRED^a

parameter	NADPH ^b	FAD ^c
k_{cat} (s ⁻¹)	10 \pm 0.5	9.0 \pm 0.5
K_M (μ M)	10 \pm 2	2.5 \pm 0.5
k_{cat}/K_M (M ⁻¹ s ⁻¹)	(1 \pm 0.2) \times 10 ⁶	(4 \pm 1) \times 10 ⁶

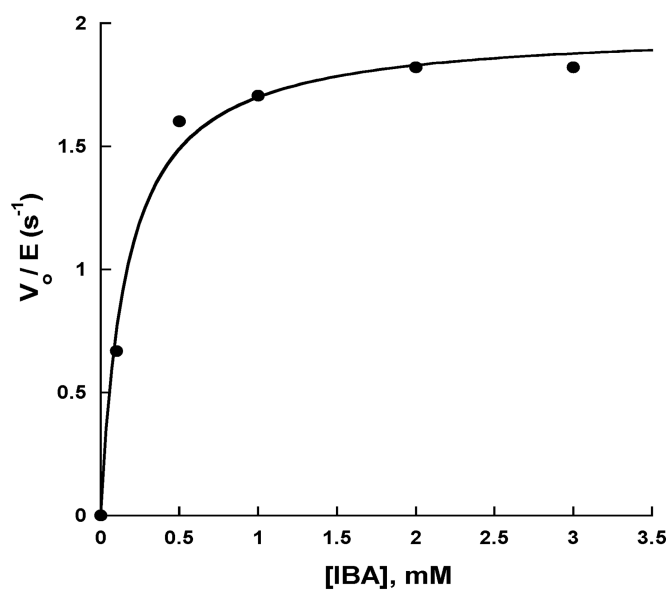
^aConditions: 100 mM sodium phosphate (pH 7.5) at 25 $^{\circ}$ C. ^bThe concentration of FAD was fixed at 30 μ M. ^cThe NADPH concentration was fixed at 200 μ M.

molecular weight of the protein was estimated to be \sim 40 kDa based on the SDS-PAGE analysis, which is consistent with the molecular weight predicted from the amino acid sequence of 39.9 kDa (Figure S1). The total protein yield was 150 mg, which represented 3.8 mg of protein per gram of cell paste. In the FRED purification, a few problems with solubility were encountered in initial trials of the purification process. These problems were mitigated by using 15% glycerol in the buffers, which greatly reduced the extent of protein aggregation. A protein with a size of \sim 21.2 kDa was observed using SDS-PAGE analysis (Figure S1). The total protein yield was 127.5 or 4.3 mg of protein per gram of cell paste.

IBAH and FRED were both purified with no bound FAD; even when FAD was added during lysis, the flavin dissociated during the purification. The polyhistidine tag bound to the recombinant proteins was not cleaved during the purification process. Protein was flash-frozen in 20 μ L aliquots of 25 mM HEPES, 150 mM NaCl, and 15% glycerol (pH 7.5) for IBAH and 25 mM HEPES, 300 mM NaCl (pH 7.5), and 15% glycerol for FRED and stored at -80 $^{\circ}$ C.

Flavin Binding to FRED. The binding of oxidized FAD (FAD_{ox}) to FRED was measured by monitoring the fluorescence change that occurred upon titration of 10 μ M

(A)



(B)

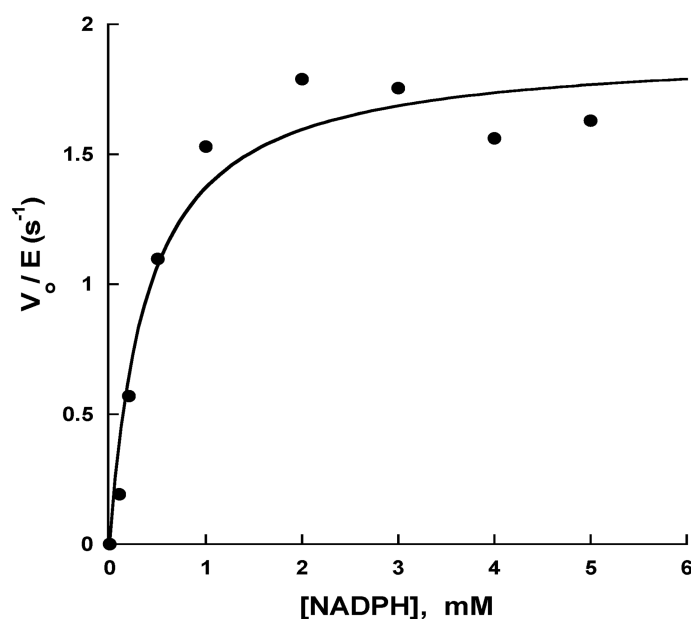


Figure 2. Oxygen consumption assay. Initial velocities as a function of (A) IBA (0.05–3 mM) and (B) NADPH (0.05–5 mM). The standard assay was performed in 100 mM sodium phosphate buffer (pH 7.5) at 25 °C. In assays in which the NADPH concentration was varied, the IBA concentration was held constant at 5 mM. In assays in which the IBA concentration was varied, 0.8 mM NADPH was present.

Table 2. Steady-State Kinetic Parameters for the FRED:IBAH System^a

parameter	oxygen consumption		product formation	
	IBA	NADPH	IBA	NADPH
k_{cat} (s ⁻¹)	1.97 ± 0.06	1.91 ± 0.10	0.024 ± 0.001	0.028 ± 0.001
K_M (μM)	200 ± 30	400 ± 100	120 ± 15	34 ± 8
k_{cat}/K_M (M ⁻¹ s ⁻¹)	(1 ± 0.2) × 10 ⁴	(5 ± 1) × 10 ³	200 ± 20	830 ± 200
coupling (%)	~1	~1		

^aConditions: 100 mM sodium phosphate buffer (pH 7.5) at 25 °C.

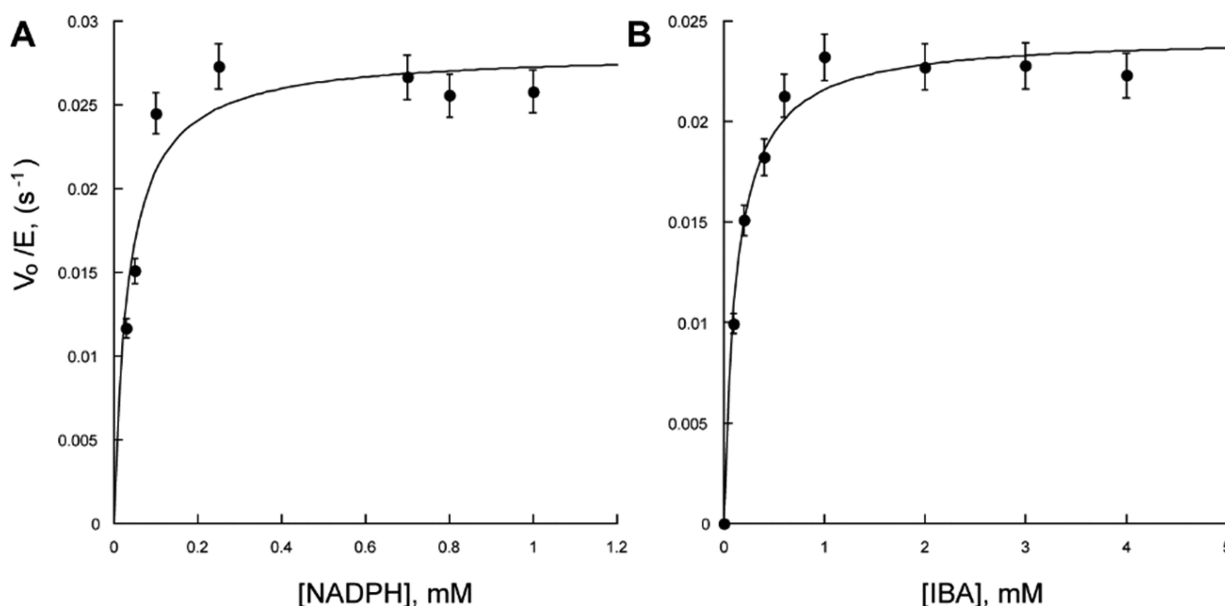


Figure 3. Product (IBHA) formation assay. (A) As a function of NADPH with FAD and IBA concentrations fixed at 10 μM and 3 mM, respectively. (B) As a function of IBA, with FAD and NADPH concentrations fixed at 10 μM and 0.8 mM, respectively.

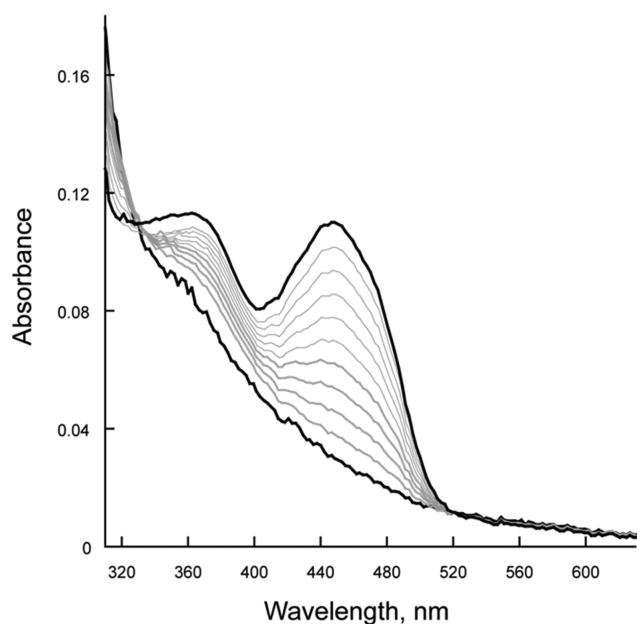


Figure 4. Flavin oxidation. Reaction of the IBAH:FAD_{red} complex with O₂ at pH 7.5 and 25 °C. Recorded UV-vis spectra of the mixture for 100 s after mixing reduced FAD with $\sim 625 \mu\text{M}$ oxygen.

FAD with FRED (0.2–70 μM). The fluorescence of FAD increased with an increase in the FRED concentration, which was interpreted as indicating binding of FAD to the enzyme (Figure 1). A similar increase in FAD fluorescence was observed with PheA2.²³ Saturation was achieved at FRED concentrations of >20 μM . The K_D of the FRED:FAD_{ox} complex was calculated to be $7.3 \pm 1.3 \mu\text{M}$.

NADPH Oxidase Activity. The oxidoreductase activity of FRED was monitored by measuring the oxidation of NADPH at 340 nm. In one experiment, the concentration of NADPH was varied (5–200 μM) and that of FAD was held constant at 30 μM . When the concentration of FAD was varied (0.5–30 μM), the concentration of NADPH was 200 μM . The initial

rate constants exhibited a hyperbolic dependence (Figure S2), allowing estimation of kinetic parameters using the Michaelis–Menten equation (Table 1). The k_{cat} is approximately 10 s^{-1} and independent of which substrate was varied. The K_M values are 10 and 2.5 μM for NADPH and FAD, respectively. Thus, the catalytic efficiencies for the two substrates are similar (within a factor of 4).

Flavin Reduction. To monitor the reduction of FAD in complex with FRED by NADPH, the absorbance change at 450 nm was monitored in the stopped-flow spectrophotometer under anaerobic conditions. The reduction of FAD bound to FRED, observed in the presence of NADPH, followed monophasic kinetics. The rate of reduction, k_{red} , was calculated as $10.0 \pm 0.25 \text{ s}^{-1}$. In the presence of IBA, the k_{red} decreased $\sim 40\%$ to $6.6 \pm 0.2 \text{ s}^{-1}$. The reaction of the FRED:FAD complex was also studied using NADH as the redox partner. The changes in absorbance at 450 nm decreased in a monophasic process, as observed for NADPH. The k_{red} with NADH was $0.35 \pm 0.03 \text{ s}^{-1}$. Thus, FRED exhibits a strong preference for NADPH over NADH.

Oxygen Consumption Assay. In assays in which the IBA concentration was varied, the background of oxygen consumption activity in the absence of IBA was subtracted from the value obtained for each concentration of IBA. In assays in which the NADPH concentration was varied, the oxygen consumption activity values obtained for each NADPH concentration, in the absence of IBAH, were subtracted from the values obtained in the presence of IBAH (Figure 2). This was done to ensure that only the activity of IBAH (instead of FRED oxidase activity) was measured under either assay condition. The k_{cat} value for oxygen consumption by the FRED:IBA system was ~ 5 times lower than the k_{cat} value for NADPH oxidation catalyzed by FRED alone (Tables 1 and 2). Also, the K_M for NADPH obtained from oxygen consumption was ~ 40 -fold higher than that from the NADPH oxidation assay. The K_M value for IBA was 200 μM .

Product Formation Assay. To quantitate the amount of IBHA produced, a variation of the Csaky iodine oxidation assay was performed.³⁰ The initial velocities for IBHA

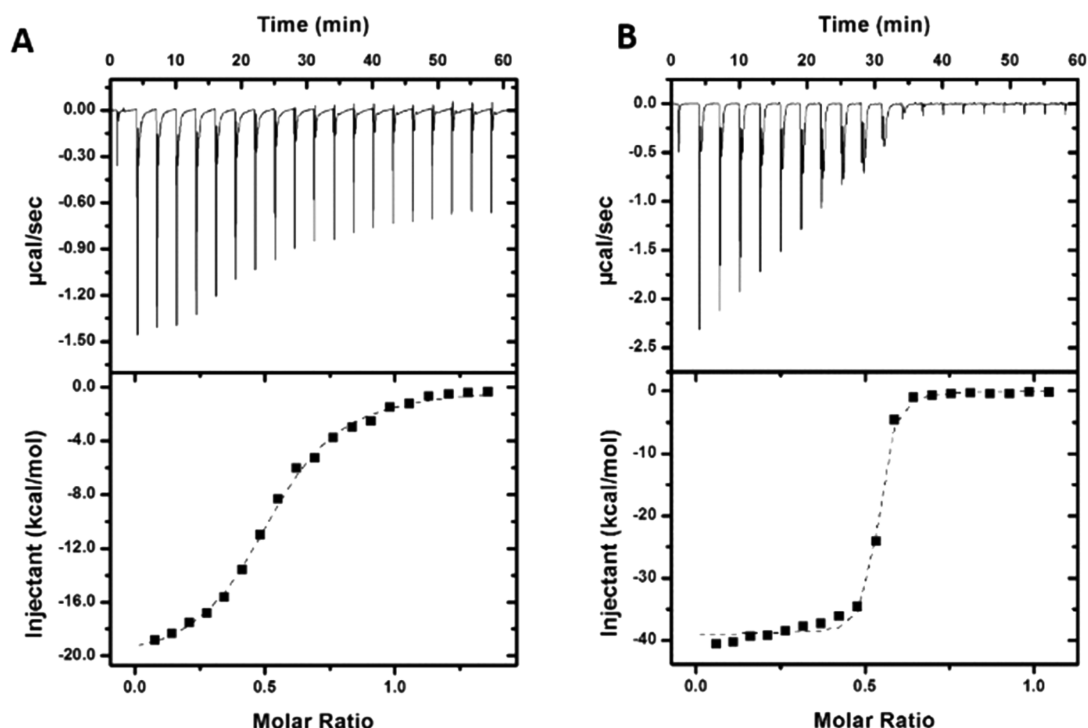


Figure 5. Measurements of the binding of FAD to FRED and IBAH by ITC. Isothermal binding curves for binding of (A) FAD_{ox} to FRED and (B) FAD_{red} to IBAH. Assay conditions: 25 mM HEPES containing 300 mM NaCl and 10% glycerol (pH 7.5) at 25 °C.

Table 3. Dissociation Constants (μM) for Ligand Binding to FRED and IBAH Determined by ITC

ligand	FRED	IBAH
FAD _{ox}	1.73 ± 0.20	38 ± 4
FAD _{ox} ^a	2.00 ± 0.17	not determined
FAD _{red}	23 ± 4	0.046 ± 0.01
NADP ⁺	5.0 ± 0.7	not determined
NAD ⁺	7.8 ± 1	not determined

^aIn the presence of 3 mM IBA.

formation were dependent on substrate concentration, as shown in Figure 3. The k_{cat} value was ~ 97 times lower than the values calculated following oxygen consumption. The K_M values for IBA and NADPH were decreased (Table 2). By taking the ratio of the k_{cat} value calculated from the oxygen consumption assay and the k_{cat} value calculated by measuring hydroxylated product, we determined that the coupling was very weak. In this case, coupling was calculated to be $\sim 1\%$; i.e., for every mole of O₂ consumed, only 0.01 mol of IBHA is produced.

Product Identification. The incorporation of oxygen into IBA was confirmed using mass spectrometry analysis. After the reaction was completed, substrate and products were derivatized to facilitate separation and detection by spectrophotometry during UPLC analysis. The elution peaks were observed at 23.48 and 27.92 min corresponding to IBHA and IBA, respectively (Figure S3). Mass spectroscopy analysis showed an ion at m/z 334.3 for the sodiated IBHA and one at m/z 350.2 for potassiated IBHA. Further analysis of the IBA peak revealed a potassiated IBA peak at m/z 334.4 and a sodiated peak at m/z 318.3 (Figure S3). The m/z difference between the potassiated IBHA and IBA peaks was m/z 16, which corresponds to one atom of oxygen (Table S1). The analysis revealed that one oxygen atom is incorporated into

IBA. The incorporation of oxygen can also be deduced for the sodiated IBHA and IBA peaks, thereby confirming that the product of the FRED:IBA reaction is a hydroxylated amine.

Flavin Oxidation. Flavin oxidation in flavin monooxygenases usually involves an initial formation and stabilization of a C4a-hydroperoxyflavin intermediate, which can be observed in the stopped-flow spectrophotometer by absorbance at ~ 380 nm. If this intermediate is not formed or stabilized, flavin oxidation occurs in a single step and no intermediate is observed. Oxidation of the IBAH:FAD_{red} complex occurred in a single step, and no intermediate was observed (Figure 4). These results suggest the C4a-hydroperoxyflavin intermediate in IBAH is not stabilized.

ITC Measurements of Ligand Binding to FRED and IBAH. The binding of FAD_{red/ox} and NAD(P)⁺ to FRED, and FAD_{red/ox} to IBAH, was measured using ITC in 25 mM HEPES containing 300 mM NaCl and 10% glycerol (pH 7.5) at 25 °C. The binding of all of these ligands was enthalpy-driven ($\Delta H < 0$). The data show that FAD_{ox} binds FRED with a similar affinity in the absence [$K_D = 1.73 \pm 0.20 \mu\text{M}$ (Figure 5A)] or presence of IBA [$K_D \sim 2 \mu\text{M}$ (Figure S4)]. The affinity of IBAH for FAD_{ox} was ~ 22 -fold lower (Table 3 and Figure S4). This trend was reversed when the reduced form of FAD was used under anaerobic conditions. The affinity of IBAH for FAD_{red} [$K_D = 46 \text{ nM}$ (Table 3 and Figure S4)] was 500-fold higher compared to that for FRED (Figure 5B). The affinities of NAD⁺ and NADP⁺ for FRED are similar ($K_D = 5\text{--}8 \mu\text{M}$) (Table 3 and Figure S4).

ITC Measurements of the Interactions between FRED and IBAH. ITC measurements were performed to observe the binding of IBAH to FRED in the presence of reduced or oxidized FAD. To prevent heat exchange from FAD binding, saturating concentrations (0.23 mM) were present in the chambers holding FRED and IBAH. The titration of IBAH with FRED in the presence of FAD_{ox} indicated that IBAH

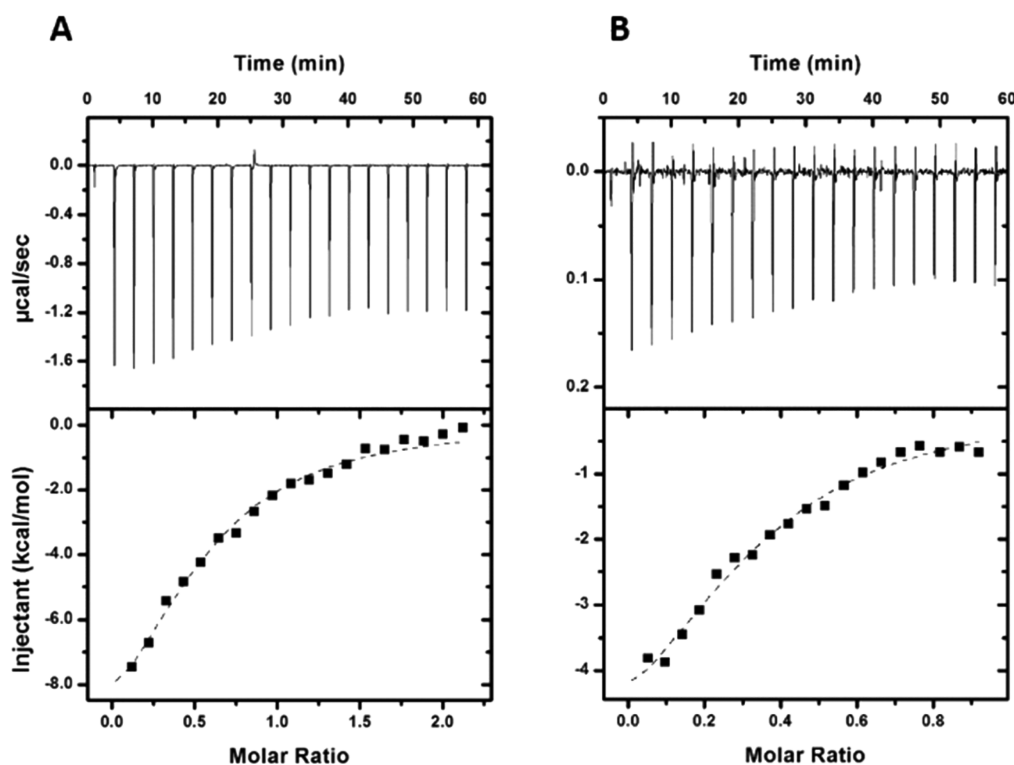


Figure 6. FRED:IBAH complex. ITC measurements for binding of (A) IBAH to the FRED:FAD_{ox} complex and (B) FRED to the IBAH:FAD_{red} complex in 25 mM HEPES containing 300 mM NaCl and 10% glycerol (pH 7.5) at 25 °C.

interacts with FRED with a K_D value of $7 \pm 1 \mu\text{M}$ (Figure 6A). The affinity of FRED for IBAH in the presence of FAD_{red} was similar ($K_D = 8.1 \pm 1.4 \mu\text{M}$) (Figure 6B). IBAH displayed no apparent affinity for FRED in the absence of FAD_{ox/red}.

DISCUSSION

In this work, we performed detailed ligand binding and kinetic characterization of the reaction of the two-component flavin-dependent monooxygenase, FRED:IBAH, from *S. viridifaciens*. We used stopped-flow spectrophotometry, isothermal titration calorimetry, and steady-state assays to gain an insight into its mechanism of action. Initially, we characterized the interaction of FRED with FAD. The K_D value for FAD was determined by monitoring the flavin fluorescence, which increases as the flavin binds to FRED. From this experiment, it was determined that FRED binds FAD_{ox} with a relatively low affinity [$\sim 7 \mu\text{M}$ (Figure 1)]. By monitoring NADPH, we determined a k_{cat} value of $\sim 10 \text{ s}^{-1}$, a K_M value of $\sim 10 \mu\text{M}$ for NADPH, and a K_M value of $2.5 \mu\text{M}$ for FAD. The k_{cat} value was ~ 5 times lower than previously reported;³¹ however, the K_M values were similar. The difference in the k_{cat} value could be associated with the presence of the His tag in the protein used in this study. Stopped-flow experiments under anaerobic conditions were used to monitor the reduction of FAD by FRED, with NADPH and NADH as co-substrates. The k_{red} value with NADPH was similar to the k_{cat} monitoring NADPH oxidation, suggesting that the hydride transfer was at least partially rate-limiting. The data also showed that FRED prefers NADPH as a co-substrate, based on a 28-fold higher k_{red} value for NADPH.

The steady-state activity of IBAH was studied by following both the consumption of oxygen and the formation of the hydroxylated product. The k_{cat} value from oxygen consumption was much higher than that obtained from the product

formation assay (1.9 s^{-1} vs 0.024 s^{-1}) (Table 2). Thus, it appears that the C4a-hydroperoxyflavin is not very stable in IBAH. This is supported by stopped-flow experiments, monitoring the changes in FAD_{red} upon reaction with oxygen, which do not show the expected formation and stabilization of an intermediate with a peak at $\sim 380 \text{ nm}$ characteristic of the C4a-hydroperoxyflavin (Figure 4). This result was somewhat unexpected, because stabilization of the C4a-hydroperoxyflavin has been observed in other class D flavin monooxygenases. These include the monooxygenase HadaA/HadB system involved in dehalogenation of chlorophenols³² and *p*-hydroxyphenylacetate-3-hydroxylase.³² The lack of C4a-hydroperoxyflavin stabilization perhaps suggests the active site of IBAH is intrinsically dynamic.³³

The affinity of FRED and IBAH for FAD_{ox} and FAD_{red} was also determined using ITC. The binding constants were consistent with the physiological substrate for each enzyme. FRED had a higher affinity for FAD_{ox} while IBAH had a much higher affinity for FAD_{red}. This binding preference has also been shown for other two-component monooxygenases.^{34–36}

Using ITC, we studied the interaction of IBAH and FRED. FRED and IBAH associate with a K_D value of $\sim 7 \mu\text{M}$ in the presence of FAD. No apparent binding was observed in the absence of FAD. These results suggest that protein conformational changes may accompany the binding of FAD to either FRED or IBAH (or both), and these conformational changes remodel the protein surfaces that mediate the FRED–IBAH interaction. The direct interaction between FRED and IBAH suggests that this monooxygenase system might use a direct flavin transfer mechanism.

In summary, the isolation of the reductase and monooxygenase components of the valanimycin biosynthetic pathway was accomplished, and the enzymes were characterized with several methods. FRED does not contain a tightly

bound flavin cofactor, prefers NADPH over NADH, and binds FAD_{ox} with a higher affinity than it binds FAD_{red}. IBAH preferentially binds FAD_{red} over FAD_{ox} and hydroxylates IBA. The IBAH hydroxylation reaction is highly uncoupled. Interaction between the two components was observed, suggesting a direct flavin transfer mechanism. This is the first detailed characterization of a two-component N-monooxygenase system involved in antibiotic biosynthesis.

■ ASSOCIATED CONTENT

Supporting Information

The Supporting Information is available free of charge at <https://pubs.acs.org/doi/10.1021/acs.biochem.0c00679>.

Figures and table with data from the purification of enzymes (IBAH and FRED), NADPH-oxidase activity of FRED, MS analysis of the IBAH product formation assay, and ITC characterization of ligand–enzyme binding (PDF)

Accession Codes

Isobutylamine N-hydroxylase, UniProt ID P96072. Flavin reductase; UniProt ID O34138.

■ AUTHOR INFORMATION

Corresponding Author

Pablo Sobrado – Department of Biochemistry and Center for Drug Discovery, Virginia Tech, Blacksburg, Virginia 24061, United States; orcid.org/0000-0003-1494-5382; Email: psobrado@vt.edu

Authors

Hao Li – Department of Biochemistry, Virginia Tech, Blacksburg, Virginia 24061, United States

Benedicta Forson – Department of Biochemistry, Virginia Tech, Blacksburg, Virginia 24061, United States

Meital Eckshtain-Levi – Department of Biochemistry, Virginia Tech, Blacksburg, Virginia 24061, United States

Hannah Valentino – Department of Biochemistry, Virginia Tech, Blacksburg, Virginia 24061, United States

Julia S. Martín del Campo – Department of Biochemistry, Virginia Tech, Blacksburg, Virginia 24061, United States

John J. Tanner – Departments of Biochemistry and Chemistry, University of Missouri, Columbia, Missouri 65211, United States; orcid.org/0000-0001-8314-113X

Complete contact information is available at:

<https://pubs.acs.org/doi/10.1021/acs.biochem.0c00679>

Funding

Research reported in this publication was supported by National Science Foundation Grants CHE-2003658 (to P.S.) and CHE-2003986 (to J.J.T.).

Notes

The authors declare no competing financial interest.

■ REFERENCES

(1) Walsh, C. T., and Wencewicz, T. A. (2013) Flavoenzymes: versatile catalysts in biosynthetic pathways. *Nat. Prod. Rep.* 30, 175–200.

(2) Romero, E., Gomez Castellanos, J. R., Gadda, G., Fraaije, M. W., and Mattevi, A. (2018) Same Substrate, Many Reactions: Oxygen Activation in Flavoenzymes. *Chem. Rev.* 118, 1742–1769.

(3) Massey, V. (2000) The chemical and biological versatility of riboflavin. *Biochem. Soc. Trans.* 28, 283–296.

(4) van Berkel, W. J., Kamerbeek, N. M., and Fraaije, M. W. (2006) Flavoprotein monooxygenases, a diverse class of oxidative biocatalysts. *J. Biotechnol.* 124, 670–689.

(5) Huijbers, M. M., Montersino, S., Westphal, A. H., Tischler, D., and van Berkel, W. J. (2014) Flavin dependent monooxygenases. *Arch. Biochem. Biophys.* 544, 2–17.

(6) Visitsatthawong, S., Chenprakhon, P., Chaiyen, P., and Surawatanawong, P. (2015) Mechanism of Oxygen Activation in a Flavin-Dependent Monooxygenase: A Nearly Barrierless Formation of C4a-Hydroperoxyflavin via Proton-Coupled Electron Transfer. *J. Am. Chem. Soc.* 137, 9363–9374.

(7) Kirchner, U., Westphal, A. H., Muller, R., and van Berkel, W. J. (2003) Phenol hydroxylase from *Bacillus thermoglucosidarius* A7, a two-protein component monooxygenase with a dual role for FAD. *J. Biol. Chem.* 278, 47545–47553.

(8) Heine, T., Tucker, K., Okonkwo, N., Assefa, B., Conrad, C., Scholtissek, A., Schlomann, M., Gassner, G., and Tischler, D. (2017) Engineering Styrene Monooxygenase for Biocatalysis: Reductase-Epoxidase Fusion Proteins. *Appl. Biochem. Biotechnol.* 181, 1590–1610.

(9) Jun, S. Y., Lewis, K. M., Youn, B., Xun, L., and Kang, C. (2016) Structural and biochemical characterization of EDTA monooxygenase and its physical interaction with a partner flavin reductase. *Mol. Microbiol.* 100, 989–1003.

(10) Chang, C. Y., Lohman, J. R., Cao, H., Tan, K., Rudolf, J. D., Ma, M., Xu, W., Bingman, C. A., Yennamalli, R. M., Bigelow, L., Babnigg, G., Yan, X., Joachimiak, A., Phillips, G. N., Jr., and Shen, B. (2016) Crystal Structures of SgcE6 and SgcC, the Two-Component Monooxygenase That Catalyzes Hydroxylation of a Carrier Protein-Tethered Substrate during the Biosynthesis of the Enediyne Antitumor Antibiotic C-1027 in *Streptomyces globisporus*. *Biochemistry* 55, 5142–5154.

(11) Kim, S. H., Hisano, T., Iwasaki, W., Ebihara, A., and Miki, K. (2008) Crystal structure of the flavin reductase component (HpaC) of 4-hydroxyphenylacetate 3-monooxygenase from *Thermus thermophilus* HB8: Structural basis for the flavin affinity. *Proteins: Struct., Funct., Genet.* 70, 718–730.

(12) Driggers, C. M., Dayal, P. V., Ellis, H. R., and Karplus, P. A. (2014) Crystal structure of *Escherichia coli* SsuE: defining a general catalytic cycle for FMN reductases of the flavodoxin-like superfamily. *Biochemistry* 53, 3509–3519.

(13) Tu, S. C. (2008) Activity coupling and complex formation between bacterial luciferase and flavin reductases. *Photochem. Photobiol. Sci.* 7, 183–188.

(14) Abdurachim, K., and Ellis, H. R. (2006) Detection of protein-protein interactions in the alkanesulfonate monooxygenase system from *Escherichia coli*. *J. Bacteriol.* 188, 8153–8159.

(15) Lei, B., and Tu, S. C. (1998) Mechanism of reduced flavin transfer from *Vibrio harveyi* NADPH-FMN oxidoreductase to luciferase. *Biochemistry* 37, 14623–14629.

(16) Ellis, H. R. (2010) The FMN-dependent two-component monooxygenase systems. *Arch. Biochem. Biophys.* 497, 1–12.

(17) Sucharitakul, J., Tinikul, R., and Chaiyen, P. (2014) Mechanisms of reduced flavin transfer in the two-component flavin-dependent monooxygenases. *Arch. Biochem. Biophys.* 555–556, 33–46.

(18) Heine, T., van Berkel, W. J. H., Gassner, G., van Pee, K. H., and Tischler, D. (2018) Two-Component FAD-Dependent Monooxygenases: Current Knowledge and Biotechnological Opportunities. *Biology (Basel, Switz.)* 7, 42.

(19) Yamato, M., Iinuma, H., Naganawa, H., Yamagishi, Y., Hamada, M., Masuda, T., Umezawa, H., Abe, V., and Hori, M. (1986) Isolation and properties of valanimycin, a new azoxy antibiotic. *J. Antibiot.* 39, 184–191.

(20) Parry, R. J., Li, W., and Cooper, H. N. (1997) Cloning, analysis, and overexpression of the gene encoding isobutylamine N-hydroxylase from the valanimycin producer, *Streptomyces viridificans*. *J. Bacteriol.* 179, 409–416.

- (21) Yamato, M., Takeuchi, T., Umezawa, H., Sakata, N., Hayashi, H., and Hori, M. (1986) Biosynthesis of valanimycin. *J. Antibiot.* 39, 1263–1269.
- (22) Guan, L. J., Lee, W. C., Wang, S., Ohshiro, T., Izumi, Y., Ohtsuka, J., and Tanokura, M. (2015) Crystal structures of apo-DszC and FMN-bound DszC from *Rhodococcus erythropolis* D-1. *FEBS J.* 282, 3126–3135.
- (23) van den Heuvel, R. H., Westphal, A. H., Heck, A. J., Walsh, M. A., Rovida, S., van Berkel, W. J., and Mattevi, A. (2004) Structural studies on flavin reductase PheA2 reveal binding of NAD in an unusual folded conformation and support novel mechanism of action. *J. Biol. Chem.* 279, 12860–12867.
- (24) Fox, B. G., and Blommel, P. G. (2009) Autoinduction of protein expression. *Current Protocols in Protein Science*, Chapter 5, Unit 5.23, Wiley.
- (25) Romero, E., Fedkenheuer, M., Chocklett, S. W., Qi, J., Oppenheimer, M., and Sobrado, P. (2012) Dual role of NADP(H) in the reaction of a flavin dependent N-hydroxylating monooxygenase. *Biochim. Biophys. Acta, Proteins Proteomics* 1824, 850–857.
- (26) Franceschini, S., Fedkenheuer, M., Vogelaar, N. J., Robinson, H. H., Sobrado, P., and Mattevi, A. (2012) Structural insight into the mechanism of oxygen activation and substrate selectivity of flavin-dependent N-hydroxylating monooxygenases. *Biochemistry* 51, 7043–7045.
- (27) Robinson, R., Badieyan, S., and Sobrado, P. (2013) C4a-hydroperoxyflavin formation in N-hydroxylating flavin monooxygenases is mediated by the 2'-OH of the nicotinamide ribose of NADP(+). *Biochemistry* 52, 9089–9091.
- (28) Csaky, T. Z., Hassel, O., Rosenberg, T., Lang (Loukamo), S., Turunen, E., and Tuhkanen, A. (1948) On the Estimation of Bound Hydroxylamine in Biological Materials. *Acta Chem. Scand.* 2, 450–454.
- (29) Chocklett, S. W., and Sobrado, P. (2010) *Aspergillus fumigatus* SidA is a highly specific ornithine hydroxylase with bound flavin cofactor. *Biochemistry* 49, 6777–6783.
- (30) Robinson, R., and Sobrado, P. (2011) Substrate binding modulates the activity of *Mycobacterium smegmatis* G, a flavin-dependent monooxygenase involved in the biosynthesis of hydroxamate-containing siderophores. *Biochemistry* 50, 8489–8496.
- (31) Parry, R. J., and Li, W. (1997) An NADPH:FAD oxidoreductase from the valanimycin producer, *Streptomyces viridifaciens*. Cloning, analysis, and overexpression. *J. Biol. Chem.* 272, 23303–23311.
- (32) Pimviriyakul, P., Thotsaporn, K., Sucharitakul, J., and Chaiyen, P. (2017) Kinetic Mechanism of the Dechlorinating Flavin-dependent Monooxygenase HadA. *J. Biol. Chem.* 292, 4818–4832.
- (33) Parry, R. J., and Li, W. (1997) Purification and characterization of isobutylamine N-hydroxylase from the valanimycin producer *Streptomyces viridifaciens* MG456-hF10. *Arch. Biochem. Biophys.* 339, 47–54.
- (34) Sucharitakul, J., Chaiyen, P., Entsch, B., and Ballou, D. P. (2006) Kinetic mechanisms of the oxygenase from a two-component enzyme, p-hydroxyphenylacetate 3-hydroxylase from *Acinetobacter baumannii*. *J. Biol. Chem.* 281, 17044–17053.
- (35) Valton, J., Filisetti, L., Fontecave, M., and Niviere, V. (2004) A two-component flavin-dependent monooxygenase involved in actinorhodin biosynthesis in *Streptomyces coelicolor*. *J. Biol. Chem.* 279, 44362–44369.
- (36) Chakraborty, S., Ortiz-Maldonado, M., Entsch, B., and Ballou, D. P. (2010) Studies on the mechanism of p-hydroxyphenylacetate 3-hydroxylase from *Pseudomonas aeruginosa*: a system composed of a small flavin reductase and a large flavin-dependent oxygenase. *Biochemistry* 49, 372–385.